AFMDC6
ISSN 1616-301X
Vol. 17, No. 1
January 5, 2007

D53313

WILEY-VCH

ADVANCED FUNCTIONAL MATERIALS

Light Emission from InGaN Epilayers

Ink-jet Printing of Nanocrystal/Polymer Composites

Organic Electronics from Organosilsesquioxanes

Deformation of Top-Down/Bottom-Up Ag Nanowires

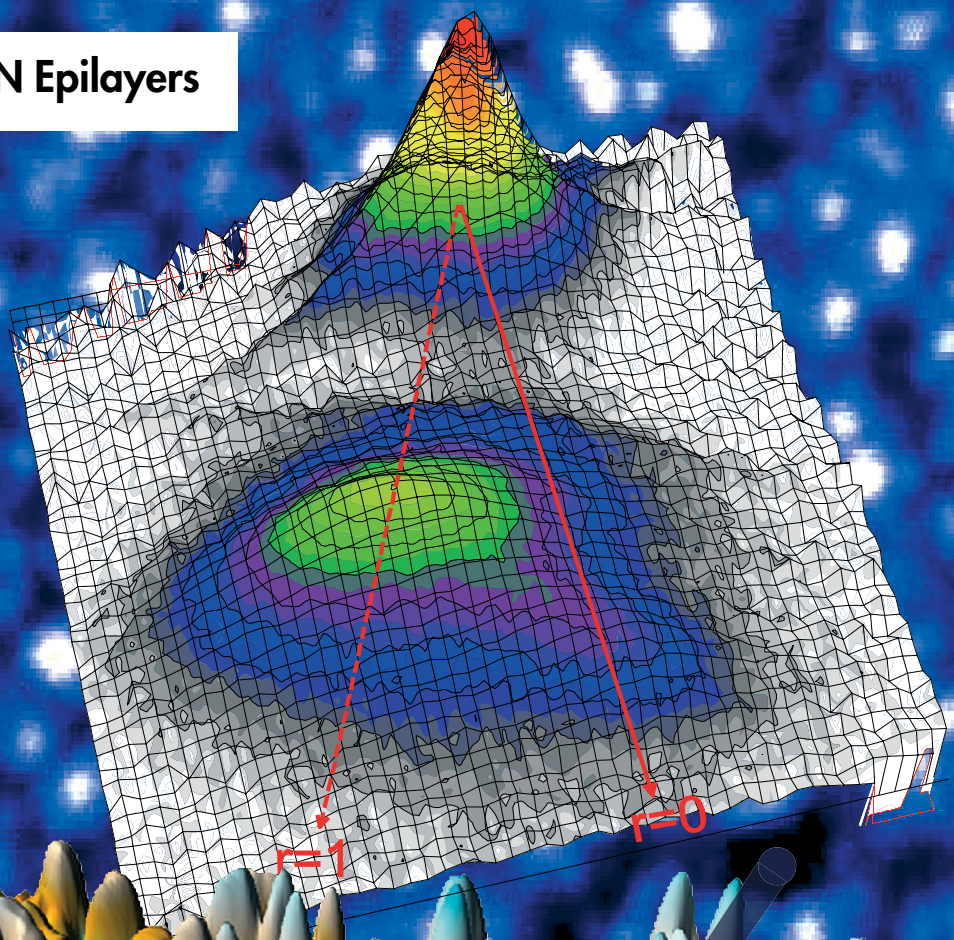

DOI: 10.1002/adfm.200600650

Role of Nanoscale Strain Inhomogeneity on the Light Emission from InGaN Epilayers**

By *Sérgio Manuel de Sousa Pereira*,* *Kevin Peter O'Donnell*, and *Eduardo Jorge da Costa Alves*

InGaN is the basis of a new generation of light-emitting devices, with enormous technological potential; it is currently one of the most intensively studied semiconductor materials. It is generally accepted that compositional fluctuations resulting from phase segregation are the origin of the high luminescence efficiency of InGaN. Evidence to show that nanoscale strain inhomogeneity plays a fundamental role in determining the spectral properties of InGaN–GaN heterostructures is reported. For layers above a certain critical thickness, a strong spatially varying strain profile accompanies a nonplanar surface morphology, which is associated with a transition from a planar 2D to a Stranski–Krastanow-like 2D–3D growth mode; the strong dependence of the critical thickness on the local InN content of the growing films drives a non-linear growth instability. Within this framework, apparently disparate experimental observations regarding structural and optical properties, previously reported for InGaN layers, are reconciled by a simple phenomenological description.

1. Introduction

Energy-efficient and environmentally friendly solid-state light sources are revolutionizing an increasing number of applications, and bring apparent benefits to vast areas of development, such as lighting, communications, biotechnology, imaging, and medicine.[1] The technological breakthrough would not have been possible without the spectacular evolution in recent years of group III nitride semiconductors, and in particular of the pseudobinary alloy, $In_xGa_{1-x}N$ (x is the InN fraction in the formula unit).[2] Although the mechanism of luminescence in this material system is not yet understood,[3–21] it has been widely suggested that its remarkable efficiency results from phase-segregation effects, related to spinodal decomposition, which have been theoretically predicted to occur in $In_xGa_{1-x}N$ for $x > 0.06$.[7] Exciton localization in InGaN has been tentatively attributed to nanometer-scale (quantum-dot-like) composition fluctuations of the alloy by several authors.[8–10]

The observation of several "anomalous" structural and optical properties has further contributed to the widespread belief that InGaN is generally a phase-segregated alloy. Experimental observations on the basis of this conception include, observation of double X-ray diffraction (XRD) peaks, observation of two-component luminescence bands and a granular-like submicrometer luminescence texture frequently observed in cathodoluminescence (CL) and confocal microscopy (CM) studies.[11–13] More directly, studies based on methods of transmission electron microscopy (TEM) have claimed experimental evidence for the presence of nanometer-sized indium-rich regions, or quantum dots (QDs), in InGaN.[8,16]

Over the last few years, much discussion about the structural and optical properties of InGaN has been constrained by a presumption of nanometer-scale phase segregation. However, so far, the experimental support for this effect has been less than decisive,[14,15] and more recent and systematic studies of InGaN clearly point out the need to re-interpret these experimental results. For example, with regard to TEM studies, several authors have recently cautioned the scientific community that electron-beam irradiation leads to the generation of an inhomogeneous strain distribution in InGaN layers that did not show pronounced compositional inhomogeneity previously.[17,18] Therefore, redistribution caused by electron-beam irradiation most likely produced artifacts in early investigations. Additionally, the observation of two InGaN related XRD peaks for various InGaN samples was shown to be uncorrelated to phase segregation.[19,20] Furthermore, it was established subsequently that samples which exhibit this structural characteristic also feature double luminescence peaks (DLPs).[21]

[*] Dr. S. Pereira
Department of Physics
Centre for Research in Ceramics and Composite Materials (CICECO)
University of Aveiro, 3810-193 Aveiro (Portugal)
E-mail: spereira@fis.ua.pt
Prof. K. P. O'Donnell
Department of Physics, Scottish Universities Physics Alliance
University of Strathclyde
Glasgow G4 0NG (UK)
Prof. E. Alves
Departamento de Física, Instituto Tecnológico e Nuclear (ITN)
Estrada Nacional. 10, 2686-953 Sacavém (Portugal)

[**] The authors acknowledge the crystal growers that have provided samples for this study; in particular Dr. Ian M. Watson from the Institute of Photonics and Dr. B. Beaumont from Lumilog. S. M. de Sousa Pereira is grateful to Dr. M. R. Correia for useful discussions and N. Franco for assistance in the XRD measurements. Financial support from Fundação para a Ciência e Tecnologia, Fundação Calouste Gulbenkian and Fundação Luso Americana para o Desenvolvimento are gratefully acknowledged.

In this contribution we address these fundamental issues regarding the microscopic nature of InGaN alloys. A detailed comparison of the optical and structural properties of a large number of InGaN–GaN bilayers, grown below and above the critical layer thickness (CLT), reveals that strong lateral and depth variations of the strain field are associated with a peculiar 2D–3D morphology in these samples. We show that this peculiar growth habit, driven by the strong dependence of the CLT on the local composition, accounts in a self-consistent manner for the observations previously considered "anomalous" and attributed without a rigorous justification to the effects of phase segregation.

2. Results and Discussion

Let us consider the photoluminescence (PL) of an InGaN light-emitting epilayer where two spectral components separated in energy by $\Delta E \sim 120$ meV can be clearly identified, as shown in Figure 1. The confocal panchromatic microscopic image shown in the inset evidences a granular "spotty" luminescence texture at a sub-micrometer length scale. The lower-energy component of this DLP is favoured when the area selected by the exciting laser is a bright spot in the confocal image. On the other hand, the higher-energy component dominates when a darker region is addressed. Bearing in mind that phase segregation was predicted to occur for $In_xGa_{1-x}N$ for $x > 0.06$, it is tempting to interpret the features observed in Figure 1 as a signature of phase segregation. In this scenario the lower-energy component would correspond to PL from the so-called "In-rich nanoclusters" or "QD-like" regions.

But what are the underlying physical parameters that determine if such spectral segregation is to appear in a given InGaN epilayer? In a systematic examination of a large number of InGaN layers grown using metal-organic chemical vapor deposition (MOCVD) we noted that observation of DLPs has been normally restricted to InGaN layers grown with a combination of certain composition and thickness (x,t) characteristics. Specifically, for a given emitting layer thickness, the lower-energy component emerges only above a critical composition and, similarly, for a given composition there is a critical thickness above which we observe double PL (and XRD) peaks. This thickness has been found to agree very well with the CLT at which strain relief starts to occur.

In a bilayer, the CLT of the adlayer can be estimated as a function of the InN content, x, by using the energy-balance method proposed by People and Bean[22]. Figure 2a shows that the CLT for $In_xGa_{1-x}N$ on GaN is a very strong function of composition, because of the rapid increase of lattice mismatch with x. The left side of the curve corresponds to the region where growth coherent to GaN is predicted, whereas

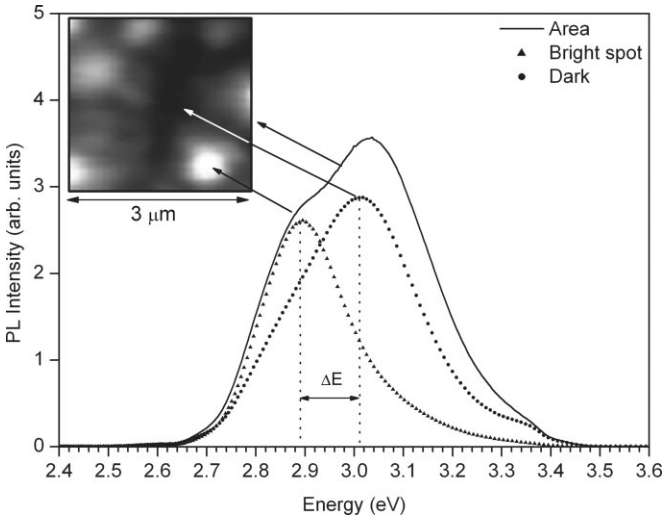

Figure 1. Microspectroscopy in an InGaN light-emitting layer illustrating a spatial and spectral "segregation" of luminescence. A two-component photoluminescence peak is revealed. The inset microscopy image identifies the sample regions selected for PL: a bright spot (relaxed 3D material), a dark region (strained 2D film), and a larger-scale area.

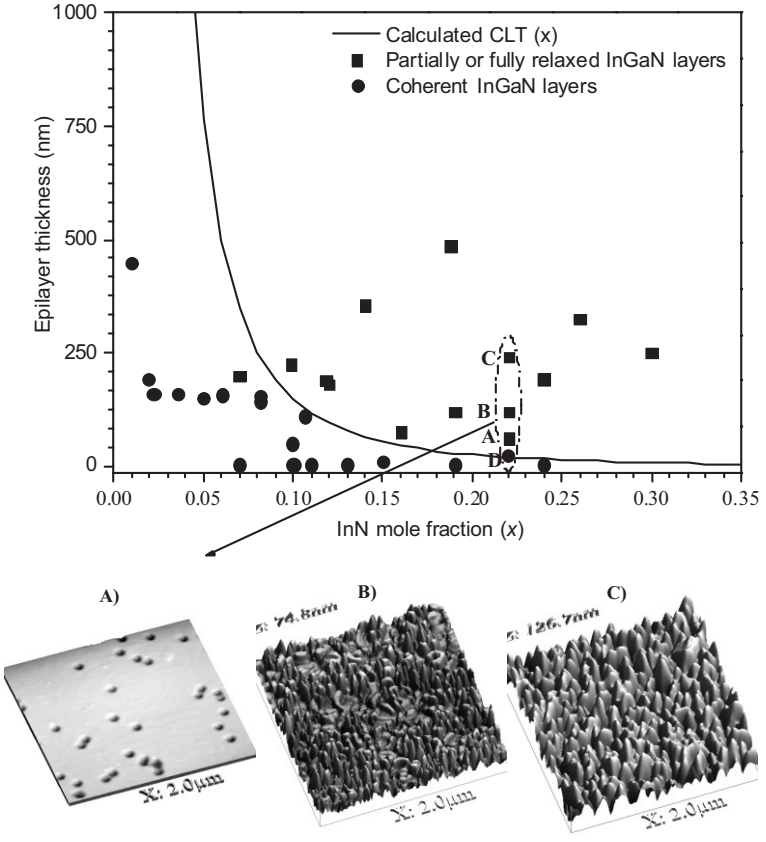

Figure 2. CLT(x), and surface morphology for $In_xGa_{1-x}N$–GaN layers. Top: Plot of the CLT(x) for strain relaxation as a function of the InN fraction and the location of the various samples studied, according to the (x,t) coordinates, relative to the calculated CLT(x). Bottom: Atomic force microscopy images (height mode) illustrating the surface morphology of the samples A, B, and C selected in Figure 2a, top.

on the right side strain relief is expected. Keeping in mind that the accuracy of this estimate is limited by the poor knowledge of the alloy elastic properties, and the approximations involved in the strain-relaxation models, the level of agreement with the early experimental measurements by Parker et al.,[23] is quite reasonable. In Figure 2a we include the much larger range of samples studied here. Samples with (x,t) values on the right side of the calculated curve typically feature: double PL peaks, double XRD peaks, and a rough 3D-like surface morphology. On the other hand, samples falling below the calculated curve generally show single luminescence and diffraction peaks and smoother surfaces.

To illustrate the evolution of a 3D surface morphology for layers grown increasingly in excess of the CLT, at a fixed composition, the AFM images of three InGaN samples (A, B, and C) selected in Figure 2a, are shown in Figure 2b. The morphology changes from a flat surface, interspersed with hexagonal pits for the thinnest sample, to a surface composed of a mixture of 2D and 3D regions for the intermediate thickness sample, and eventually to a very rough surface dominated by large (sub-micrometer) 3D islands for the layer grown well above the CLT for that value of x.

It is well known that misfit accommodation in strained epitaxial systems can take place through the onset of islanding and general surface roughness.[24] Often the growth-mode transition from layer-by-layer growth to 3D islanding occurs quite abruptly when a certain critical strain state is reached. The latter, so-called Stranski–Krastanow (SK) transition has been observed for several strained layer systems (e.g., SiGe and GaAs–InGaAs).[24] It appears that a similar effect occurs spontaneously in InGaN–GaN, and, because of the very large lattice mismatch of ca. 10 % between InN and GaN, it leads to very strong lateral and depth variations of the strain field associated with such peculiar mixed 2D–3D growth mode on a nanometer length scale.

In order to gain an insight into the strain-relaxation process and to understand its correlation with the 2D–3D growth morphology a detailed high-resolution XRD study was performed. The asymmetric reciprocal space maps (RSMs) of the (10–15) diffraction patterns, obtained for samples a–c, is shown in Figure 3. Symmetric RSMs were also performed and evidenced a perfect alignment between the $In_{0.22}Ga_{0.78}N$ and GaN reciprocal lattice points (RLPs), indicating that there are no macroscopic tilts between film and buffer.

The results in Figure 3 demonstrate that the maximum of the InGaN RLP progressively shifts from a fully strained ($r = 0$) to a fully relaxed ($r = 1$) position as the layer thickness increases (from a–c). It appears that all InGaN layers start growing nearly pseudomorphic to GaN and do not relax uniformly (as a whole) along the growth direction. Even sample c, which is mostly fully relaxed (maximum of RLP coincides with the full relaxation line), remains partly coherent to the GaN buffer. In fact, by considering the relative intensities in the region near the $r = 1$ line from a–c, we may infer that further growth leads to an increasing fraction of relaxed material in the layer. Therefore, it is suggested that the 3D growth mechanism results in elastically relaxed InGaN. In order to test this correlation we have resorted to a chemical-etching process, and the thickness of sample c (240 nm) was reduced to about 30 nm, leaving only the 2D part of the film; the XRD RSM obtained for this sample is shown in Figure 3d. After removal of the 3D-like near-surface region, the RSM is identical to that obtained for the thinnest (2D) film shown in Figure 3a. This result evidences clearly the relationship between the 3D growth and strain relaxation.

Taking into account what we have learned about the nanostructure of InGaN layers grown with thicknesses larger than the CLT, for a given composition, let us now try to establish direct correlations between optical and structural properties. The first relationship to unveil is that the size of the bright regions typically observed in spatially resolved CL studies,[9,11,13] and also in Figure 1 (which is responsible for the lower-energy PL component), is identical to the lateral sizes of the islands observed in AFM microscopic images. The second important issue is the energy splitting, ΔE, typically observed. To provide a general overview, the values of ΔE observed in the samples studied here and in several other works from the literature, were plotted together in Figure 4. The trend, which indicates that ΔE would appear to vanish as x approaches zero, is striking. The magnitude of strain variation between coherent and relaxed components decreases with x, and any strain-induced shift should therefore disappear as x (ε_{xx}) tends to zero. In order to provide an additional insight regarding the close link between surface morphology, nanoscale strain inhomogeneity, and emission energy it is appropriate to pursue a phenomenological description which may account for the ΔE results, as a function of x, summarized in Figure 4. First, to make it possible to compare different data points from the literature, we rely on the relation between PL peak energy and x for MOCVD-grown $In_xGa_{1-x}N$ layers obtained in the low InN content ($x < 0.3$) range: $E_{PL} = 3.398 - 3.91\,x$ eV.[25]

Knowing x, one can estimate the variation between extreme states of strain corresponding to fully coherent (2D) and fully relaxed (3D) layer regions. Since the parallel strain component, ε_{xx}, equals zero for relaxed material composing the islands, the upper limit of strain variation for a given composition, $\Delta\varepsilon_{xx}$, is

$$\Delta\varepsilon_{xx} \simeq (a_0^{InGaN} - a^{GaN})/a_0^{InGaN} \quad (1)$$

where a_0^{InGaN} is the relaxed InGaN lattice constant as given by Vegard's law

$$a_0^{InGaN} = x\,a_0^{InN} + (1-x)\,a_0^{GaN} \quad (2)$$

with $a_0^{GaN} = 0.3189$ nm[26] and $a_0^{InN} = 0.3538$ nm[27]). This approximation assumes compositional uniformity along the growth direction. In the samples discussed here one can ensure (using Rutherford backscattering spectrometry (RBS) and RSM analysis) that there are no substantial "compositional pulling effects" such as previously reported in some InGaN samples.[28] However, one should be aware that under certain growth conditions differences in x between the 2D and 3D regions may occur, breaking down the previous assumption.

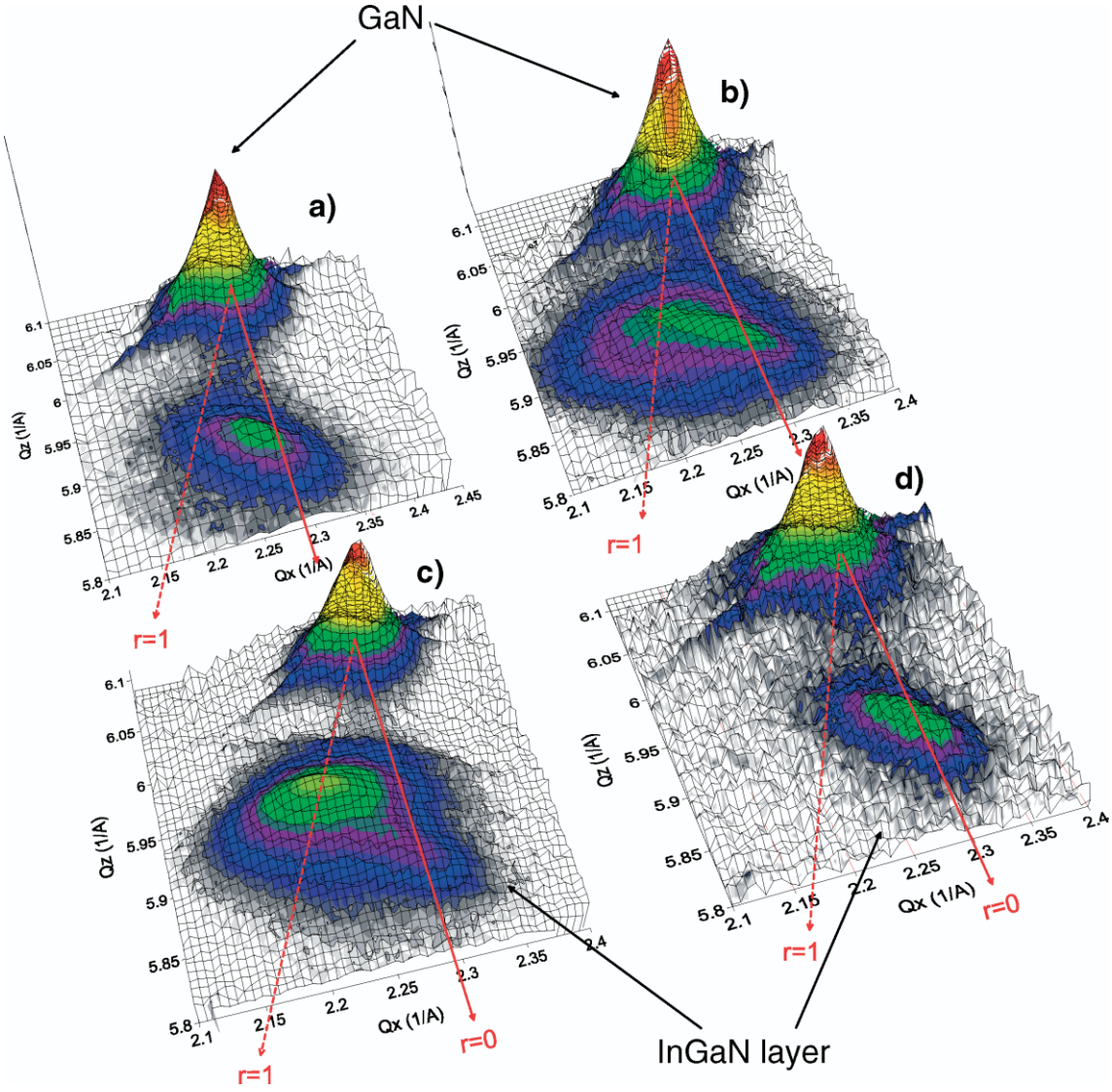

Figure 3. XRD reciprocal space mapping of the (10.5) reflections of InGaN–GaN. Layers with thickness below (d), close to (a,b), and well above (c) the CLT, as indicated in Figure 2. The map shown in (d) corresponds to sample (c) after a surface etching. The full lines passing through the GaN buffer layer RLP indicate coherent InGaN, that is, relaxation ($r=0$), whereas the dashed lines ($r=1$) correspond to fully relaxed InGaN.

The strain inhomogeniety causes a variation in the bandgap energy (E_g) which, in a first-order approximation, is proportional to $\Delta\varepsilon_{xx}$: $\Delta E = \text{coef.}_{xx} * \Delta\varepsilon_{xx}$, where coef._{xx} is the proportionality coefficient. The only unknown to calculate ΔE from a given emission energy is the parallel strain coefficient, coef._{xx}. Thus, we may set it as an adjustable parameter, and let it vary in a fitting procedure. The best fit to data in Figure 4 is obtained with $\text{coef.}_{xx} = -8.7 \pm 0.8$ eV.

At the current state of knowledge, it is not possible to compare this value of strain coefficient with theoretical estimates. A comparison with independent measurements or with theory will be possible when a credible estimate or experimental value for the InN strain deformation potentials, required to estimate those of InGaN, is available. However, the exciton transition energies of GaN have been measured with good precision as a function of in-plane strain (ε_{xx}) by Shan et al.[29] From the data provided in the literature[29] a $\text{coef.}_{xx}(\text{GaN}) = -9.3$ eV can be determined by a linear least-squares fitting to the A-exciton energy. If we take into account the fact that we are performing our analysis on the low x range, it is indeed quite reasonable that the strain coefficients of InGaN and GaN should be found to be similar.

This last is a rather significant result. It evidences that the description proposed, which entails a strong correlation between surface morphology, nanoscale strain, and PL emission energy, describes our results, and those reported in the literature. These findings cast stringent doubts regarding the validity of the common assumption of phase segregation, together with the existence of structural phase-separated "nanoclusters" or "In-rich QDs". The nanoscale strain inhomogeneity model presented here comprehensively treats experimental results on single InGaN films found in the literature.

ADVANCED FUNCTIONAL MATERIALS

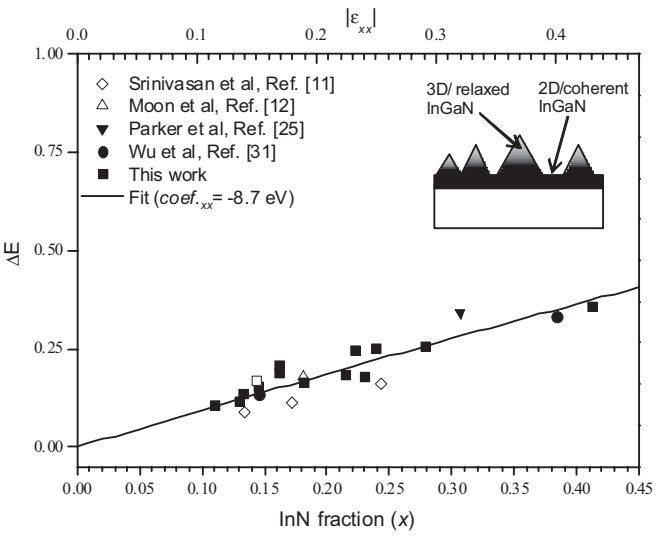

Figure 4. Plot of luminescence energy splitting ΔE, as a function of the InN fraction. The parallel strain (ε_{xx}) variation, between relaxed InGaN (3D islands) and coherent InGaN (2D) layer regions, is schematically illustrated in the inset. The graph includes results obtained in this work and several other results taken from the literature. The line represents the fit obtained considering the model proposed.

Although the physical problem for InGaN–GaN QW structures (where strong polarization effects and quantum-confinement effects are present) is more complex than the case of the single layers studied here, double PL peaks may also be found in multiple quantum well (MQW) structures with an energy correlation that follows the model proposed here.[30,31] The bandgap energy difference caused by a local variation between fully relaxed and strained material in a QW appears to be still proportional to the InN content in the well region in these cases. For MQWs, the strain relaxation, when it is verified, may have a different nature from the 3D growth with a pronounced islanding (SK-like) growth mode verified for thicker layers. The thickness–composition regime for a local strain relaxation is also expected to be distinct; in the MQW, preferential sites for such local strain relaxation are likely to be close to dislocations and V pits. In fact, it is rather interesting to note that Wu et al.[30] observed a long-wavelength shoulder on the MQW InGaN–GaN emission when probing a wedge-shaped plan-view TEM sample using CL. The relative intensity of the lower-energy peak increased when the region close to the V pits was preferentially probed.

3. Conclusions

A systematic investigation that combined conventional and microspectroscopy, AFM, and high-resolution XRD, carried out on a wide range of samples, evidences the fundamental role of nanoscale strain inhomogeneity on the optical and structural properties of InGaN–GaN layers. The presence of strong lateral and depth variations of the strain field is shown to be associated with a transition in the growth mode from planar 2D to an SK-like 2D–3D. This work attempts to unify several experimental observations commonly reported in InGaN epilayers, namely, the (sub-micrometer) length scale of the granular-like luminescence texture, the observation of double XRD peaks, and the emergence of secondary lower-energy PL components. Additionally, the energy splitting observed in the PL spectra can be quantitatively accounted for by a nanostructure-based phenomenological description that considers the strain effect on the band structure. Given that most experimental results on the basis of the common assumption of nanometer-scale phase segregation in InGaN could be explained in this way, it seems desirable that other conceptual routes, which do not overlook the effects of strain on the length scale of the expected compositional fluctuations, should be developed to better understand the physics of this fascinating material system.

4. Experimental

The samples studied here are nominally undoped wurtzite InGaN–GaN layers, grown using MOCVD on *c*-plane Al_2O_3 substrates provided by several laboratories around the world including: the Institute of Photonics (IOP) of the University of Strathclyde, Aixtron AG, Thomson-CSF, and the University of Ghent. Standard InGaN growth conditions for IOP are described in the literature [32]. Surface etchings were performed in a melt of NaOH–KOH, on the eutectic point at 230 °C for 60 s. The eutectic etch performed here has been used previously to reveal defects in GaN epilayers [33]. PL was excited with the He–Cd laser and spatially resolved (lateral resolution ca. 100 nm) spectroscopy and microscopy was performed at the Daresbury scanning confocal microscope, SYCLOPS. High-resolution XRD was performed in a double-crystal diffractometer equipped with a position sensitive detector placed on the 2θ arm. The instrumental angular resolution is ca. 30 s of arc. RBS measurements were performed to determine the $In_xGa_{1-x}N$ composition and thickness, with a 1 mm collimated beam of 2.0 MeV $^4He^+$.

Received: July 21, 2006
Final version: September 25, 2006
Published online: November 24, 2006

[1] N. Nadarajah, *Phys. World* **2005**, *July*, 18.
[2] *Low-Dimensional Nitride Semiconductors* (Ed: B. Gil), Oxford University Press, Oxford **2002**.
[3] S. Nakamura, *Science* **1998**, *281*, 956.
[4] S. Pereira, M. R. Correia, T. Monteiro, E. Pereira, E. Alves, A. D. Sequeira, N. Franco, *Appl. Phys. Lett.* **2001**, *78*, 2137.
[5] J. Wu, W. Walukiewicz, K. M. Yu, J. W. Ager, III, E. E. Haller, H. Lu, W. J. Schaff, *Appl. Phys. Lett.* **2002**, *80*, 4741.
[6] K. P. O'Donnell, S. Pereira, R. W. Martin, P. R. Edwards, M. J. Tobin, J. F. W Mosselmans, *Phys. Status Solidi A* **2003**, *195*, 532.
[7] I. Ho, G. B.Stringfellow, *Appl. Phys. Lett.* **1996**, *68*, 2701.
[8] Y. Narukawa, Y. Kawakami, M. Funato, S. Fujita, S. Fujita, S. Nakamura, *Appl. Phys. Lett.* **1997**, *70*, 981.
[9] S. Chichibu, K. Wada, S. Nakamura, *Appl. Phys. Lett.* **1997**, *71*, 2346.
[10] K. P. O'Donnell, R. W. Martin, P. G. Middleton, *Phys. Rev. Lett.* **1999**, *82*, 237.
[11] S. Srinivasan, F. Bertram, A. Bell, F. A. Ponce, S. Tanaka, H. Omiya, Y. Nakagawa, *Appl. Phys. Lett.* **2002**, *80*, 550.
[12] Y.-T. Moon, D.-J. Kim, J.-Su. Park, J.-Ta. Oh, J.-M. Lee, Y.-W. Ok, H. Kim, Se.-J. Park, *Appl. Phys. Lett.* **2001**, *79*, 599.
[13] H. J. Chang, C. H. Chen, Y. F. Chen, T. Y. Lin, L. C. Chen, K. H. Chen, Z. H. Lan, *Appl. Phys. Lett.* **2005**, *86*, 021 911/1-3.
[14] S. Pereira, M. R.Correia, E. Alves, K. P. O'Donnell, *Appl. Phys. Lett.* **2005**, *87*, 136 101/1-2.

[15] K. P. O'Donnell, R. W. Martin, S. Pereira, *Appl. Phys. Lett.* **2002**, *81*, 1353.
[16] L. Nistor, H. Bender, A. Vantomme, M. F. Wu, J. Van Landuyt, K. P. O'Donnell, R. Martin, K. Jacobs, I. Moerman, *Appl. Phys. Lett.* **2000**, *77*, 507.
[17] T. Li, E. Hahn, D. Gerthsen, A. Rosenauer, A. Strittmatter, L. Reissmann, D. Bimberg, *Appl. Phys. Lett.* **2005**, *86*, 241 911.
[18] a) T. M. Smeeton, M. J. Kappers, J. S. Barnard, M. E. Vickers, C. J. Humphreys, *Appl. Phys. Lett.* **2003**, *83*, 5419. b) A. Rosenauer, D. Gerthsen, V. Potin, *Phys. Status Solidi A* **2006**, *203*, 176.
[19] S. Pereira, M. R. Correia, E. Pereira, K. P. O'Donnell, E. Alves, A. D. Sequeira, N. Franco, *Appl. Phys. Lett.* **2001**, *79*, 1432.
[20] S. Pereira, M. R. Correia, E. Pereira, K. P. O'Donnell, E. Alves, A. D. Sequeira, N. Franco, I. M. Watson, C. J. Deatcher, *Appl. Phys. Lett.* **2002**, *80*, 3913.
[21] S. Pereira, M. R. Correia, E. Pereira, C. Trager-Cowan, F. Sweeney, K. P. O'Donnell, E. Alves, N. Franco, A. D. Sequeira, *Appl. Phys. Lett.* **2002**, *81*, 1207.
[22] R. People, J. C. Bean, *Appl. Phys. Lett.* **1985**, *47*, 322.
[23] C. A. Parker, J. C. Roberts, S. M. Bedair, M. J. Reed, S. X. Liu, N. A. El-Masry, *Appl. Phys. Lett.* **1999**, *75*, 2776.
[24] *Low-Dimensional Semiconductor Structures* (Eds: K. Barnham, D. Vvedensky), Cambridge University Press, London **2001**.
[25] R. W. Martin, P. R. Edwards, K. P. O'Donnell, E. G .Mackay, I. M. Watson, *Phys. Status Solidi A* **2002**, *192*, 117.
[26] T. Detchprohm, K. Hiramatsu, K. Itoh, I. Akasaki, *Jpn. J. Appl. Phys. Part 2* **1992**, *31*, L1454.
[27] W. Paszkowicz, *Powder Diffr.* **1999**, *14*, 258.
[28] S. Pereira, M. R. Correia, E. Pereira, E. Alves, C. Trager-Cowan, K. P. O'Donnell, *Phys. Rev. B: Condens. Matter Mater. Phys.* **2001**, *64*, 205 311.
[29] W. Shan, T. J. Schmidt, R. J. Hauenstein, J. J. Song, B. Goldenberg, *Phys. Rev. B: Condens. Matter Mater. Phys.* **1996**, *54*, 13 460.
[30] X. H. Wu, C. R. Elsass, A. Abare, M. Mack, S. Keller, P. M. Petroff, S. P. DenBaars, J. S. Speck, S. J. Rosner, *Appl. Phys. Lett.* **1998**, *72*, 692.
[31] W. Lu, D. B. Li, C. R. Li, Z. Zhang, *J. Appl. Phys.* **2004**, *96*, 5267.
[32] C. J. Deatcher, C. Liu, S. Pereira, M. Lada, A. G. Cullis, Y. J. Sun, O. Brandt, I. M. Watson, *Semicond. Sci. Technol.* **2003**, *18*, 212.
[33] J. L. Weyher, P. D. Brown, J. L. Rouviere, T. Wosinski,. A. R. A. Zauner, I. Grzegory, *J. Cryst. Growth* **2000**, *210*, 151.